PROCEEDINGS OF SCIENCE

Study of charged current decays at LHCb

Abhijit Mathad, on behalf of the LHCb collaboration[a,*]

[a] *European Organisation for Nuclear Research (CERN), Esplanade des Particules 1, 1211 Geneva 23, Switzerland*

E-mail: amathad@cern.ch

Semileptonic charged current decays, particularly $b \to c\ell^-\bar{\nu}_\ell$ and $b \to u\ell^-\bar{\nu}_\ell$ processes, have played a pivotal role in testing the foundations of the Standard Model of particle physics. This report presents recent findings from the LHCb experiment, where these decays have been explored to investigate three critical fronts: lepton flavor universality, the pursuit of new physics phenomena beyond the Standard Model, and the precision constraints imposed on the Cabibbo-Kobayashi-Maskawa matrix elements $|V_{cb}|$ and $|V_{ub}|$.

16th International Conference on Heavy Quarks and Leptons (HQL2023)
28 November-2 December 2023
TIFR, Mumbai, Maharashtra, India

*Speaker

PoS(HQL2023)029

1. Introduction

Within the framework of the Standard Model (SM) of particle physics, charged current transitions represent tree-level processes that result in changes in the flavor of quarks and leptons, accompanied by the emission of an off-shell W boson. A notable example of such a process is the $b \to c\ell^-\bar{\nu}_\ell$ transition, where ℓ represents a lepton and $\bar{\nu}_\ell$ is the corresponding anti-neutrino. This transition is depicted in Figure 1.

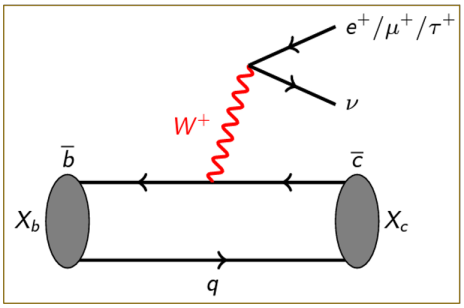

Figure 1: Feynman diagram illustrating the $b \to c\ell^-\bar{\nu}_\ell$ transition.

There are several advantages to studying charged current b-quark transitions within the LHCb experiment. Firstly, the large production cross-section of b-hadrons at the LHC and the high branching fraction (BF) of $b \to c\ell\nu$ transitions, on the order of 10^{-2}, facilitate the collection of a substantial number of decays, resulting in high statistical precision in the measurements. Secondly, the theoretical significance of this process is underlined by its capability to separate long-distance effects, represented by form factors, from short-distance effects, encapsulated by Wilson coefficients.

While the exploration of these decays offers promising avenues, it is not without its challenges. One of the primary obstacles is the issue of missing neutrinos, which significantly compromises the resolution of the measured kinematic observables. Additionally, the presence of substantial and diverse partially reconstructed backgrounds adds layers of complexity to the analysis. To address these challenges, one also requires large and precisely calibrated simulation samples to accurately model both the signal and background processes.

In previous studies, semileptonic charged current decays, specifically $b \to c\ell^-\bar{\nu}_\ell$ and $b \to u\ell^-\bar{\nu}_\ell$ processes, have been extensively utilised to investigate a wide range of phenomena. These investigations encompass the exploration of production properties of both b-hadrons and c-hadrons, the examination of neutral b-meson mixing characteristics, and the analysis of decay properties such as branching fractions and form factors. Furthermore, these decay modes have served as valuable tools for probing lepton flavor universality that is discussed in Section 2, searching for potential new physics effects beyond the SM that is discussed in Section 3, and constraining the Cabibbo-Kobayashi-Maskawa (CKM) matrix elements, specifically $|V_{cb}|$ and $|V_{ub}|$, that is discussed in Section 4. The summary and conclusions are presented in Section 5.

2. Lepton flavour universality tests

In the Standard Model (SM), the couplings of the electroweak force to leptons are flavor universal, with the exception of the Yukawa couplings of the Higgs boson. However, new physics

models can introduce interactions that violate lepton flavor universality, leading to an enhancement of the decay rate of one lepton flavor over another. These models predict that the decay rates related to the third generation of leptons will be particularly affected [12, 13].

One observable that is sensitive to such new physics effects is the lepton flavor universality (LFU) ratio, which is defined as the ratio of the branching fractions of $b \to c\tau^-\overline{\nu}_\tau$ and $b \to c\mu^-\overline{\nu}_\mu$ and is given by:

$$R(X_c) = \frac{\mathcal{BF}(X_b \to X_c\tau^-\overline{\nu}_\tau)}{\mathcal{BF}(X_b \to X_c\mu^-\overline{\nu}_\mu)}, \tag{1}$$

where X_b and X_c represent b and c mesons, respectively. The LFU ratio offers several advantages as an observable, primarily due to its theoretical cleanliness. In particular, the uncertainties associated with form factors and CKM matrix elements largely cancel out in this ratio. Additionally, the common systematic uncertainties related to detection efficiencies and yield estimation from data also cancel out.

At LHCb the LFU ratio is measured using two different tau (τ) decay modes: semimuonic and hadronic τ decays. The decay $\tau \to \mu X$ has a BF of approximately 17.4%, featuring a final state that is shared between the signal and the semimuonic normalisation channel. This decay mode is complicated by the presence of multiple missing neutrinos, necessitating the use of a boost approximation to infer the B meson momentum by its proportionality to the visible momentum ($p_B^{\parallel} \propto p_{vis}^{\parallel}$). On the other hand, the decay $\tau \to 3\pi(\pi^0)$ has a combined BF of around 13.5%, and the LFU ratio for this decay is particularly sensitive to external inputs of BF. A fully reconstructed hadronic decay is used for normalisation, such as $B \to D^*3\pi$. For this decay, a better resolution can be achieved by inferring the B momentum, albeit with a two-fold ambiguity.

The latest results from LHCb exploring semimuonic tau decays are presented in Ref. [4]. This study focuses on the LFU ratios $R(D^*)$ and $R(D)$ utilising data from Run 1, which comprises 3 fb^{-1}. The signal processes investigated are $B^0 \to D^{*+}\tau^-\bar{\nu}_\tau$, $B \to D^{*0}\tau^-\bar{\nu}_\tau$, and $B^- \to D^0\tau^-\bar{\nu}_\tau$. It is critical to isolate the signal from feed-down contributions such as $B \to D^{**}l^-\nu$ and double charm processes, for example, $B \to D^{(*)}DX$. To achieve this isolation techniques and 3D template fit is conducted using variables such as di-lepton invariant mass squared q^2 (with 4 bins), square of the missing mass m^2_{miss}, and energy of the lepton in the B rest frame E^*_l. A simultaneous fit is performed on 8 samples: 2 signal and 6 control regions, with the latter being instrumental for data-driven background modelling. The fit result in one of the signal regions in a particular q^2 bin is shown in Figure 2.

The latest results from LHCb exploring hadronic tau decays are presented in Ref. [5]. In this analysis measurement of LFU ratio $R(D^*)$ is conducted using data from partial Run 2, which includes 2 fb^{-1}. The signal process under scrutiny is $B^0 \to D^{*+}\tau^-\bar{\nu}_\tau$. A two-tiered approach is employed to reduce backgrounds: prompt background from $B^0 \to D^{*+}3\pi \pm X$ is reduced by requiring the τ vertex downstream of the B meson decay vertex, and double charm background from $B^0 \to D^{*+}D_s(\to 3\pi^\pm X)$ is minimised using an anti-D_s Boosted Decision Tree (BDT). The analysis methodology includes a 3D template fit to the squared momentum transfer q^2, the anti-D_s BDT output, and the τ lifetime. To refine the background modelling, two dedicated control regions are defined for $B^0 \to D^{*+}D_s^+X$. The fit result in the signal region is shown in Figure 3.

Both the results from LHCb [4, 5] are combined by the HFLAV group [8] to obtain world averages of the LFU ratios $R(D^*)$ and $R(D)$, which is shown in Figure 4. The systematic uncertainties

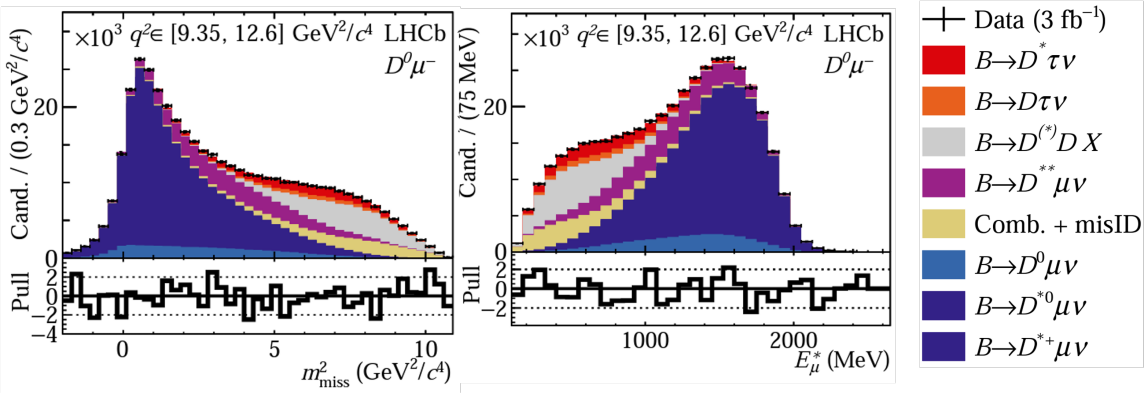

Figure 2: Fit result from the analysis of semimuonic tau decay in one of the two signal regions in a particular q^2 bin with a range of $9.35 < q^2 < 12.6$ GeV^2 [4].

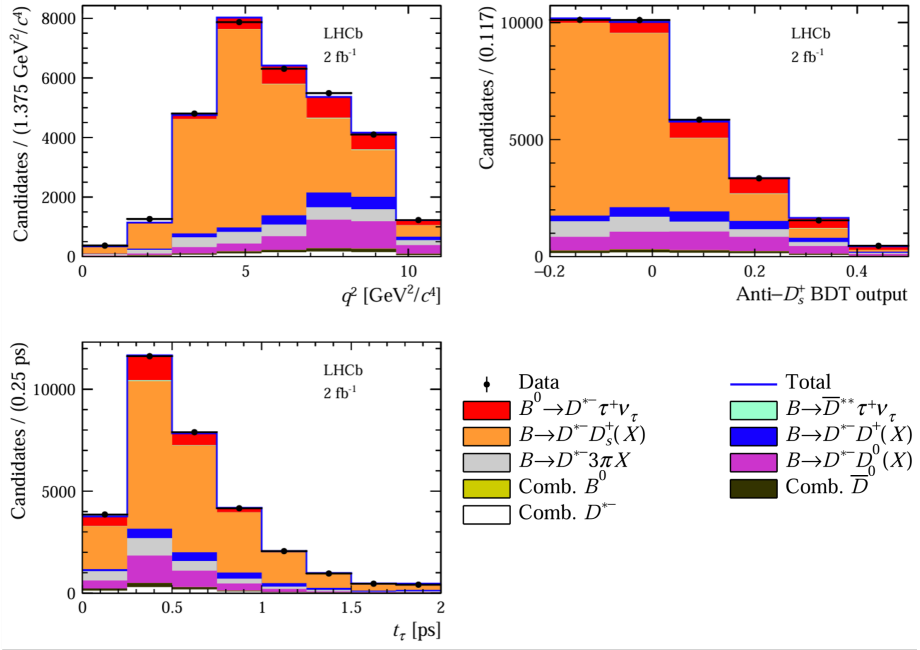

Figure 3: Fit result from the analysis of hadronic tau decays in the signal region [5].

on both of the measurements are dominated by the size simulation samples and limited knowledge in the modelling of the background processes. The world average exhibits a deviation from the SM prediction at the level of 3.3 standard deviations. It should be noted that there exist several tensions in the SM prediction of $R(D^*)$ pertaining to the form factors of $B \to D^*$ decays, which are discussed in Ref. [6, 16].

3. New physics searches

Motivated by the discrepancies observed in LFU measurements, the LHCb experiment has undertaken exploration beyond mere branching fraction ratios. This involves a investigation into the kinematic distributions of the final state particles, which possess a heightened sensitivity to

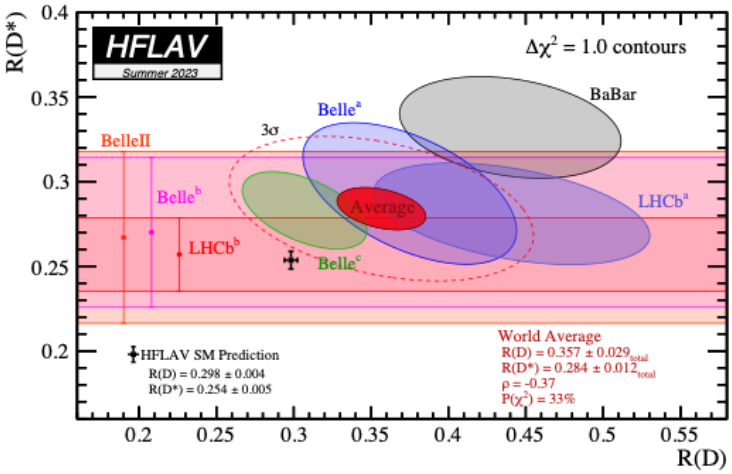

Figure 4: World average of the LFU ratios $R(D^*)$ and $R(D)$ [8].

potential NP effects. These observables have the capacity to reveal substantial deviations from SM predictions, even in scenarios where LFU ratios align with SM expectations.

A recent measurement from LHCb in Ref. [2] explores measurement of the longitudinal polarisation fraction $F_L^*(q^2)$ of the D^* meson in the decay $B^0 \to D^{*+}\tau^-\bar{\nu}_\tau$, utilising data sets from Run 1 ($3\ fb^{-1}$) and partial Run 2 ($2\ fb^{-1}$). The $F_L^*(q^2)$ distribution is extremely sensitive to the presence of NP [7]. The differential decay of $B^0 \to D^{*+}\tau^-\bar{\nu}_\tau$ and the longitudinal polarisation fraction $F_L^*(q^2)$ are given by

$$\frac{d^2\Gamma}{dq^2 d\cos\theta_D} = a_{\theta_D}(q^2) + c_{\theta_D}(q^2)\cos^2\theta_D \tag{2}$$

$$F_L^*(q^2) = \frac{a_{\theta_D}(q^2) + c_{\theta_D}(q^2)}{3a_{\theta_D}(q^2) + c_{\theta_D}(q^2)} \tag{3}$$

where $a_{\theta_D}(q^2)$ and $c_{\theta_D}(q^2)$ are functions that are proportional to the unpolarized and polarised D^* decays, respectively. The number of polarised and unpolarized D^* decays are measured by exploiting the angular distribution $\cos(\theta_D)$, which is defined as the angle between the D^0 meson and the B^0 meson in the D^* rest frame. The fit projection of the $\cos(\theta_D)$ distribution is shown in Figure 5.

The analysis strategy very closely follows the hadronic $R(D^*)$ analysis [5] with an additional fine-tuning of $cos(\theta_D)$ observable for background modes using data-driven techniques. The study measures $F_L^*(q^2)$ in two bins of q^2 up to and beyond 7 GeV^2 and the results are shown in Figure 6. The systematic uncertainties related to the measurements of $F_L^*(q^2)$ are dominated by the size of the simulation samples and the limited knowledge of the background processes.

4. Measurement of $|V_{cb}|$ and $|V_{ub}|$

Within the SM framework, the strength of quark flavor transitions is described by the Cabibbo-Kobayashi-Maskawa (CKM) matrix, which is a unitary matrix. Accurate determination of $|V_{cb}|$

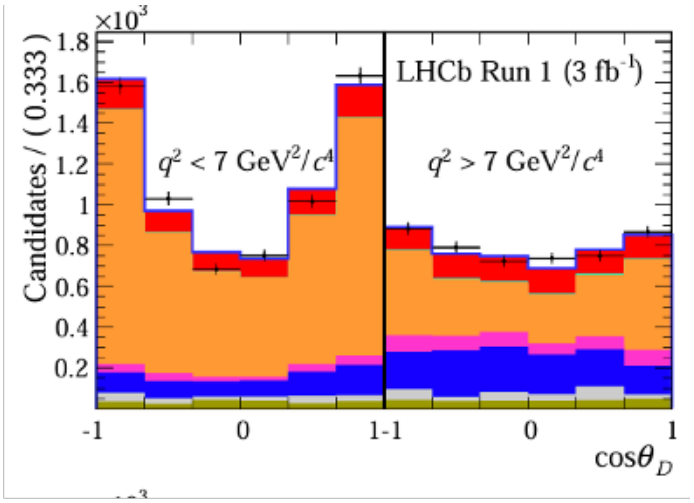

Figure 5: Fit projection of the $\cos(\theta_D)$ distribution in the $B^0 \to D^{*+}\tau^-\bar{\nu}_\tau$ analysis.

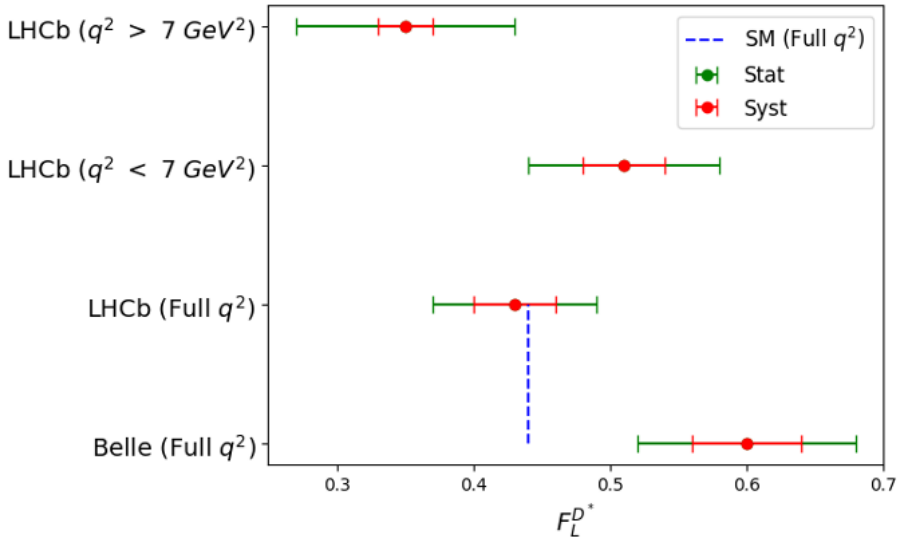

Figure 6: Measurement of the longitudinal polarisation fraction $F_L^*(q^2)$.

and $|V_{ub}|$ is crucial for constraining the sides and apex of the CKM unitarity triangle, reflecting CP violation in the quark sector. Moreover there is longstanding tension at the level of 4.1 standard deviations between the measurements of $|V_{cb}|$ and $|V_{ub}|$ from inclusive and exclusive decays, which is discussed in Ref. [8]. Therefore it is imperative to measure these quantities using a variety of decay modes and techniques.

A recent LHCb measurement [3] lead to the extraction of $|V_{cb}|$ from the decays of $B_s^0 \to D_s^{(*)-}\mu^+\nu_\mu$. This analysis utilises data from Run 1 ($3\ fb^{-1}$) and employs a normalisation channel $B^0 \to D^{(*)-}\mu^+\nu_\mu$. Here the $D^-_{(s)}$ mesons are reconstructed in the $\phi(\to K^+K^-)\pi^-$ final states. To measure $|V_{cb}|$ and the related hadronic form factors the analysis explores the differential decay rates

given by

$$\frac{d\Gamma(B_s^0 \to D_s^- \mu^+ \nu_\mu)}{dw} = \frac{G_F^2 |V_{cb}|^2}{48\pi^3} m_{D_s}^3 (m_{B_s} + m_{D_s})^2 (w^2 - 1)^{3/2} \eta_{\rm EW}^2 |f_+(w)|^2 \tag{4}$$

and

$$\frac{d\Gamma(B_s^0 \to D_s^{*-} \mu^+ \nu_\mu)}{dw d\cos\theta_\mu d\cos\theta_{D_s} d\chi} = \frac{3 m_{B_s}^3 m_{D_s^*}^2 G_F^2 |V_{cb}|^2}{16(\pi)^4} \eta_{\rm EW}^2 |A(w, \theta_\mu, \theta_{D_s}, \chi)|^2 \tag{5}$$

where w is the velocity transfer, θ_μ, θ_{D_s}, and χ are the decay angles, and $\eta_{\rm EW}$ is the electroweak correction factor. The functions $f_+(w)$ and $A(w, \theta_\mu, \theta_{D_s}, \chi)$ include dependence on the hadronic form factors. In this analysis both Caprini-Lellouch-Neubert (CLN) [11] and Boyd-Grinstein-Lebed (BGL) [10] parametrizations are used to model the form factors.

To extract $|V_{cb}|$ and the associated form factors the analysis performs a 2D template fit to the corrected mass $m_{\rm corr} = \sqrt{m^2(D_s\mu) + p_\perp^2(D_s\mu)}$ and the perpendicular momentum $p_\perp(D_s)$ distributions as shown in Figure 7. The $m_{\rm corr}$ distribution is used to achieve a good separation between signal and background, while the $p_\perp(D_s)$, which is defined as the perpendicular momentum component of D_s relative to the B meson's flight direction, has a strong dependence on the form factors.

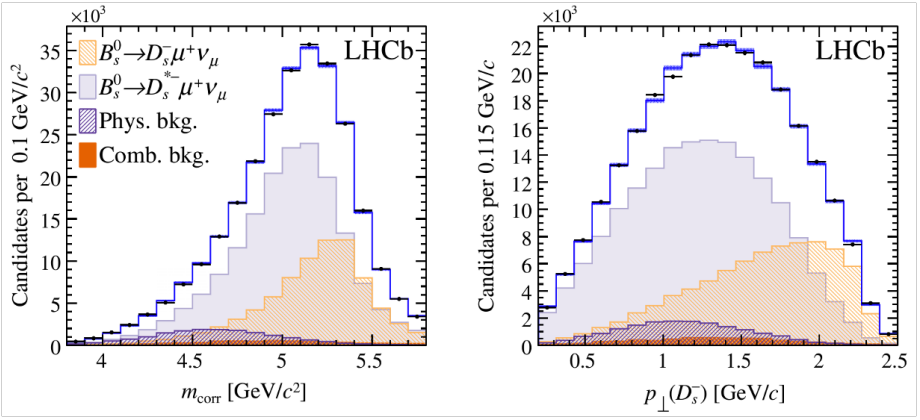

Figure 7: Fit result from the $B_s^0 \to D_s^{(*)-} \mu^+ \nu_\mu$ analysis in the $m_{\rm corr}$ and $p_\perp(D_s)$ distributions.

The results of the $|V_{cb}|$ measurement from B_s^0 decays represent the first measurement of $|V_{cb}|$ with the B_s^0 system. Form factors are parameterised using the CLN and BGL models, yielding $|V_{cb}|_{\rm CLN} = (41.4 \pm 0.6({\rm stat}) \pm 0.9({\rm syst}) \pm 1.2({\rm ext})) \times 10^{-3}$ and $|V_{cb}|_{\rm BGL} = (42.3 \pm 0.8({\rm stat}) \pm 0.9({\rm syst}) \pm 1.2({\rm ext})) \times 10^{-3}$. The primary systematic uncertainties arise from external inputs, particularly the fragmentation fractions f_s/f_d and the branching fraction of the normalisation channel. Figure 8 shows a comparison of the $|V_{cb}|$ measurements from B_s^0 decays with previous measurements from B^0 decays.

The LHCb experiment has also performed a measurement of $|V_{ub}|$ from the decay $B_s^0 \to K^- \mu^+ \nu_\mu$ [1] using data from Run 1 ($3\ fb^{-1}$). The normalisation channel is $B_s^0 \to D_s^- \mu^+ \nu_\mu$, with D_s^- being reconstructed from $K^+ K^- \pi^-$. The experimentally determined ratio of branching fractions for the signal and normalisation channels is related to $|V_{ub}|$ and $|V_{cb}|$, modulated by the form factors

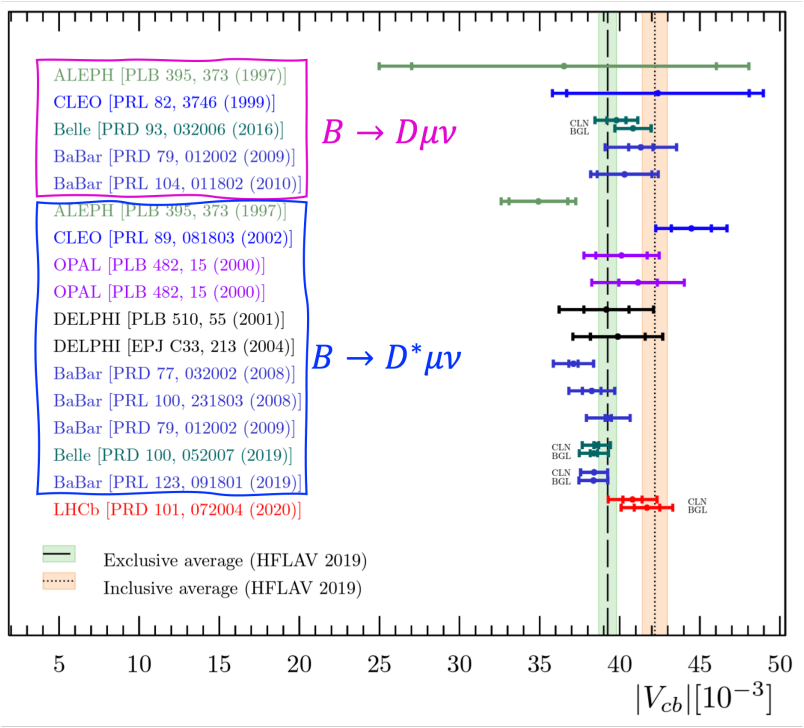

Figure 8: Comparison of the $|V_{cb}|$ measurements from B_s^0 decays with previous measurements from $B^{0,\pm}$ decays.

FF_K and FF_{D_s} as shown in Equation 6.

$$\frac{\mathcal{BF}(B_s^0 \to K^-\mu^+\nu_\mu)}{\mathcal{BF}(B_s^0 \to D_s^-\mu^+\nu_\mu)} = \frac{|V_{ub}|^2}{|V_{cb}|^2}\frac{FF_K(q^2)}{FF_{D_s}(q^2)} \tag{6}$$

The signal decay is analysed in two q^2 bins, each up to and beyond 7 GeV^2, to accommodate different theoretical form factor inputs. To extract the signal yield, a 1D template fit is performed to the corrected mass m_{corr} distribution as shown in Figure 9. This fit yields $N = 6922 \pm 285$ signal events in the low q^2 region and $N = 6399 \pm 370$ signal events in the high q^2 region.

This analysis forms the first extraction of the ratio $|V_{ub}|/|V_{cb}|$ using the B_s system. The results in the low q^2 region are $|V_{ub}|/|V_{cb}|_{\text{low}} = 0.0607 \pm 0.0015(\text{stat}) \pm 0.0013(\text{syst}) \pm 0.0008(\text{FF}) \pm 0.0030(\text{FF}_{D_s})$, and in the high q^2 region $|V_{ub}|/|V_{cb}|_{\text{high}} = 0.0946 \pm 0.0030(\text{stat}) \pm 0.0024(\text{syst}) \pm 0.0013(\text{FF}) \pm 0.0068(\text{FF}_{D_s})$. Here the first uncertainty is statistical, the second is systematic, the third is related to the form factor FF_K, and the fourth is related to the form factor FF_{D_s}. Systematic uncertainties are dominated by the modelling of signal and background, particularly form factor variations and the modelling of $B \to cc(\bar{\mu}\mu)KX$ background.

Both the low and high q^2 regions are inconsistent with each other due the underlying disagreement between the form factors used in the two regions. In the low q^2 region the form factors are taken from light cone sum rules [17], while in the high q^2 region the form factors are taken from lattice QCD [9]. It is noteworthy that the previous lattice QCD form factor determinations of $B_s^0 \to K$ decays [9] have been superseded by more recent lattice determinations [14, 15], however

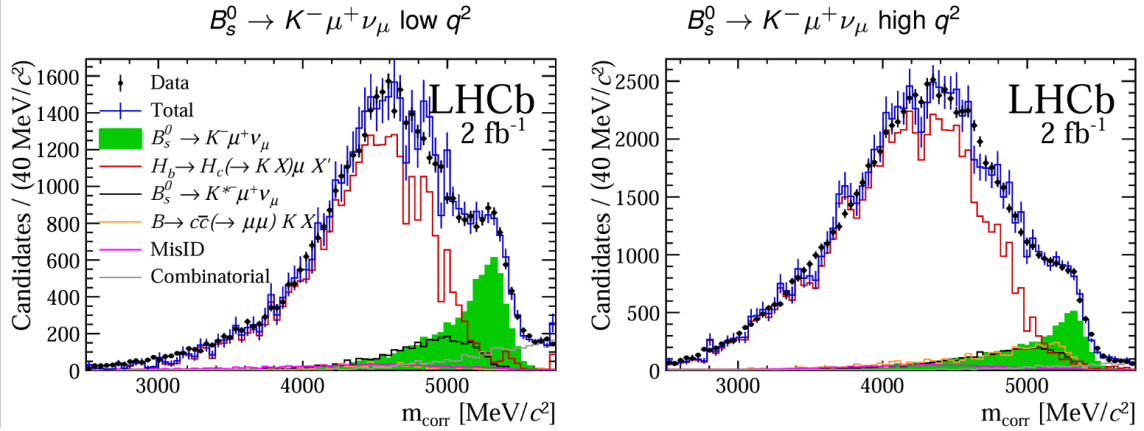

Figure 9: Fit result from the $B_s^0 \to K^-\mu^+\nu_\mu$ analysis in the $m_{\rm corr}$ distribution.

this does not resolve the tension between the $|V_{ub}/V_{cb}|$ determinations in the low and high q^2 regions.

5. Summary and conclusion

These decays are crucial for investigating lepton flavor universality, probing for signs of new physics, and refining our understanding of the Cabibbo-Kobayashi-Maskawa (CKM) matrix elements, $|V_{cb}|$ and $|V_{ub}|$.

There are also several ongoing LHCb analyses, which are expected to be completed in the near future. These include measuring Lepton Flavor Universality (LFU) ratios such as $R(D^+)$, $R(D^{*0})$, and $R(\Lambda_c^+)$; conducting new physics searches through angular analyses and precise form factor measurements; and determining $|V_{cb}|$ and $|V_{ub}|$ by studying decays such as $\Lambda_b^0 \to \Lambda_c^+\mu^-\bar{\nu}_\mu$, $B^+ \to \pi^+\mu^-\bar{\nu}_\mu$, and $B_c^+ \to D^{*0}\mu^+\nu_\mu$.

Looking ahead, the LHCb experiment is set to continue its data collection in Run 3 and beyond. This extended period of research will allow for the exploration of additional suppressed decay modes, particularly those involving $b \to u\ell^-\bar{\nu}_\ell$ transitions, and will enhance the precision of existing measurements.

References

[1] R. Aaij et al. First observation of the decay $B_s^0 \to K^-\mu^+\nu_\mu$ and Measurement of $|V_{ub}|/|V_{cb}|$. *Phys. Rev. Lett.*, 126(8):081804, 2021.

[2] R. Aaij et al. Measurement of the D^* longitudinal polarization in $B^0 \to D^{*-}\tau^+\nu_\tau$ decays. 11 2023.

[3] Roel Aaij et al. Measurement of $|V_{cb}|$ with $B_s^0 \to D_s^{(*)-}\mu^+\nu_\mu$ decays. *Phys. Rev. D*, 101(7):072004, 2020.

[4] Roel Aaij et al. Measurement of the ratios of branching fractions $\mathcal{R}(D^*)$ and $\mathcal{R}(D^0)$. *Phys. Rev. Lett.*, 131:111802, 2023.

[5] Roel Aaij et al. Test of lepton flavor universality using B0→D*-τ+$\nu\tau$ decays with hadronic τ channels. *Phys. Rev. D*, 108(1):012018, 2023.

[6] I. Adachi et al. Determination of |Vcb| using B¯0→D*+$\ell-\nu^{-}\ell$ decays with Belle II. *Phys. Rev. D*, 108(9):092013, 2023.

[7] Ashutosh Kumar Alok, Dinesh Kumar, Suman Kumbhakar, and S Uma Sankar. D^* polarization as a probe to discriminate new physics in $\bar{B} \to D^*\tau\bar{\nu}$. *Phys. Rev. D*, 95(11):115038, 2017.

[8] Y. Amhis et al. Averages of b-hadron, c-hadron, and τ-lepton properties as of 2021. *Phys. Rev. D*, 107:052008, 2023.

[9] Alexei Bazavov et al. $B_s \to K\ell\nu$ decay from lattice QCD. *Phys. Rev. D*, 100(3):034501, 2019.

[10] C. Glenn Boyd, Benjamin Grinstein, and Richard F. Lebed. Precision corrections to dispersive bounds on form-factors. *Phys. Rev. D*, 56:6895–6911, 1997.

[11] Irinel Caprini, Laurent Lellouch, and Matthias Neubert. Dispersive bounds on the shape of anti-B —> D(*) lepton anti-neutrino form-factors. *Nucl. Phys. B*, 530:153–181, 1998.

[12] Svjetlana Fajfer, Jernej F. Kamenik, and Ivan Nisandzic. On the $B \to D^*\tau\bar{\nu}_\tau$ Sensitivity to New Physics. *Phys. Rev. D*, 85:094025, 2012.

[13] Svjetlana Fajfer and Nejc Košnik. Vector leptoquark resolution of R_K and $R_{D^{(*)}}$ puzzles. *Phys. Lett. B*, 755:270–274, 2016.

[14] J. M. Flynn, R. C. Hill, A. Jüttner, A. Soni, J. T. Tsang, and O. Witzel. Exclusive semileptonic Bs→K$\ell\nu$ decays on the lattice. *Phys. Rev. D*, 107(11):114512, 2023.

[15] J. M. Flynn, A. Jüttner, and J. T. Tsang. Bayesian inference for form-factor fits regulated by unitarity and analyticity. 3 2023.

[16] Judd Harrison. Talk at LHCb 2023 implications workshop Lattice QCD Predictions for Charged Current Decays. https://indico.cern.ch/event/1258750/contributions/5606234/attachments/2740989/4767883/Lattice_QCD_Predictions_for_Charged_Current_Decays.pdf, 2023.

[17] Alexander Khodjamirian and Aleksey V. Rusov. $B_s \to K\ell\nu_\ell$ and $B_{(s)} \to \pi(K)\ell^+\ell^-$ decays at large recoil and CKM matrix elements. *JHEP*, 08:112, 2017.